Journal of Cerebral Blood Flow & Metabolism (2014) 34, 228–234

www.jcbfm.com

ORIGINAL ARTICLE

Impaired cerebrovascular hemodynamics are associated with cerebral white matter damage

Sushmita Purkayastha[1,2,3], Otite Fadar[3,4], Aujan Mehregan[4], David H Salat[3,5,6], Nicola Moscufo[3,7], Dominik S Meier[3,7], Charles RG Guttmann[3,7], Naomi DL Fisher[3,8], Lewis A Lipsitz[1,2,3] and Farzaneh A Sorond[1,3,4]

White matter hyperintensities (WMH) in elderly individuals with vascular diseases are presumed to be due to ischemic small vessel diseases; however, their etiology is unknown. We examined the cross-sectional relationship between cerebrovascular hemodynamics and white matter structural integrity in elderly individuals with vascular risk factors. White matter hyperintensity volumes, fractional anisotropy (FA), and mean diffusivity (MD) were obtained from MRI in 48 subjects (75 ± 7years). Pulsatility index (PI) and dynamic cerebral autoregulation (dCA) was assessed using transcranial Doppler ultrasound of the middle cerebral artery. Dynamic cerebral autoregulation was calculated from transfer function analysis (phase and gain) of spontaneous blood pressure and flow velocity oscillations in the low (LF, 0.03 to 0.15 Hz) and high (HF, 0.16 to 0.5 Hz) frequency ranges. Higher PI was associated with greater WMH ($P<0.005$). Higher phase across all frequency ranges was associated with greater FA and lower MD ($P<0.005$). Lower gain was associated with higher FA in the LF range ($P=0.001$). These relationships between phase and FA were significant in the territories limited to the middle cerebral artery as well as across the entire brain. Our results show a strong relationship between impaired cerebrovascular hemodynamics (PI and dCA) and loss of cerebral white matter structural integrity (WMH and DTI metrics) in elderly individuals.

Journal of Cerebral Blood Flow & Metabolism (2014) **34,** 228–234; doi:10.1038/jcbfm.2013.180; published online 16 October 2013

Keywords: aging; cerebral white matter; DTI; dynamic cerebral autoregulation; TCD

INTRODUCTION

Cerebral white matter injury, seen as regions of white matter hyperintensity (WMH) on T2-weighted magnetic resonance imaging (MRI) sequences, is a significant correlate of cognitive decline and slowing of gait in elderly people.[1,2] These white matter changes, which are also strongly associated with vascular risk factors, are regarded as typical MRI expressions of small vessel disease.[3,4] However, the histopathologic correlates of WMH are quite heterogeneous and include chronic cerebral ischemia, demyelination, venous collagenosis, edema, and microcystic infarcts.[5–8] Little is known about the precise mechanisms leading to these diverse changes in the cerebral white matter.

A number of studies have shown a strong relationship between impairments in cerebrovascular hemodynamics such as vasoreactivity and pulsatility index (PI) and WMH.[9–11] Pathologic evidence supports the relationship between aspects of small vessel disease, such as decreased vascular density, tortuous arterioles, and deposition of excessive collagen in veins, with WMH.[7,12] Some of the possible mechanisms of small vessel disease include altered cerebral autoregulation, blood–brain barrier leakage, lipohyalinosis-related narrowing of lumen, venous collagenosis, oxidative stress, inflammation, and degeneration.[7,13] Given the prevalence of vascular disease and the significant impact of white matter damage on motor and cognitive decline as well as the prevalence of stroke, it is paramount that we continue to probe the relationship between cerebrovascular hemodynamics and WMH using novel imaging and analytical tools.

Diffusion tensor imaging (DTI) of the cerebral white matter can detect early age-related changes in normal-appearing white matter (NAWM), which are not evident on a conventional MRI and may precede the development of WMH.[14,15] Although volumetric measures of WMH may be more representative of the global and cumulative effects of multiple pathologic processes, early changes may help identify causal mechanisms responsible for cerebral white matter injury.[16] Animal models have shown that impaired cerebral autoregulation is apparent months before the first histologic evidence of white matter injury.[17] Therefore DTI measures may provide important information about the relation between cerebral vascular function and white matter structural integrity early in the course of white matter injury and at a time when interventions might be most effective. Therefore, our study was designed to examine the cross-sectional relationship between cerebrovascular hemodynamics and MRI measures of cerebral white matter structural integrity in elderly individuals with vascular risk factors. We specifically studied two measures of cerebrovascular hemodynamics, pulsatility index (PI), a measure of cerebrovascular compliance), and dynamic cerebral autoregulation (dCA),

[1]Institute for Aging Research, Hebrew SeniorLife, Boston, Massachusetts, USA; [2]Division of Gerontology, Beth Israel Deaconess Medical Center, Boston, Massachusetts, USA; [3]Harvard Medical School, Boston, Massachusetts, USA; [4]Department of Neurology, Stroke Division, Brigham and Women's Hospital, Boston, Massachusetts, USA; [5]MGH/MIT/HMS Athinoula A. Martinos Center for Biomedical Imaging, Department of Radiology, Massachusetts General Hospital, Boston, Massachusetts, USA; [6]Boston VA Healthcare System, Neuroimaging Research for Veterans Center, Boston, Massachusetts, USA; [7]Center for Neurological Imaging, Department of Radiology, Brigham and Women's Hospital, Boston, Massachusetts, USA and [8]Department of Medicine, Division of Endocrinology, Diabetes and Hypertension, Brigham and Women's Hospital, Boston, Massachusetts, USA. Correspondence: Dr S Purkayastha, Institute for Aging Research, Hebrew SeniorLife, 1200 Centre Street, Boston, MA 02131, USA.
E-mail: sushmitapurkayastha@hsl.harvard.edu
This work was supported by NIH grants T32 AG23480 (SP), RO1HL089570 (NDLF), R01 NR010827 (DHS), P01 AG004390 (LAL) and R37 AG025037 (LAL), K23 AG030967 (FAS).
Received 24 July 2013; revised 11 September 2013; accepted 12 September 2013; published online 16 October 2013

and their relationship with WMH volume and DTI measures (fractional anisotropy (FA) and mean diffusivity (MD)) in NAWM.

MATERIALS AND METHODS

Forty-eight subjects (75 ± 7 years) with vascular risk factors were enrolled in this study. Subjects had either hypertension (determined by either systolic arterial blood pressure ⩾ 140 mm Hg or diastolic blood pressure ⩾ 90 mm Hg on repeated occasions or treatment with antihypertensive treatment) or well-controlled type 2 diabetes or both (Table 1). All subjects were screened with a medical history, followed by a physical examination and ECG. Doppler ultrasound of the intracranial vessels was performed and subjects with distinct hemispheric asymmetries or focal stenoses were excluded from the study. Subjects with history of stroke and transient ischemic attacks were also excluded. The Institutional Review Boards of the Brigham and Women's Hospital and Hebrew SeniorLife approved this study. All subjects provided written informed consent. The study protocol required 2 days of participation, one visit for the MRI acquisition and the other visit for cerebrovascular measurements.

Brain Imaging

Volumes of WMH normalized by intracranial volume were estimated from the MRI. Diffusion tensor imaging measures of global FA and MD in NAWM were also acquired. The DTI metrics are computed from the molecular diffusion of protons present in water molecules within the tissues. Structural properties such as fiber tract orientation, myelin structure and density, and axonal structure influence this diffusion. Animal models have reported correlations between DTI changes and histologic markers of axon and myelin structural integrity.[18] Therefore, the DTI metrics are an indirect measurement of tissue structural integrity. Higher FA and lower MD are associated with greater tissue integrity.

Table 1. Demographics and baseline characteristics of the subjects

Subject characteristics	N = *48*
Demographics	
Age (years) (mean ± s.d.)	75 ± 7
Women % (*n*)	46 (22)
Whites % (*n*)	85 (41)
Diabetes % (*n*)	44 (21)
Hypertension % (*n*)	69 (33)
Medications % (n)	
Angiotensin II receptor blockers	17 (8)
ACE inhibitors	30 (14)
Calcium channel blockers	19 (9)
Beta blockers	31 (15)
Diuretics	46 (22)
Statins	60 (29)
Neuroimaging (mean ± s.d.)	
White matter hyperintensity normalized by ICV (%)	1.0 ± 0.7
Fractional anisotropy in normal WM	0.4 ± 0.05
Mean diffusivity in normal WM (μm^2/second)	0.82 ± 0.06
Physiologic measures (mean ± s.d.)	
Systolic blood pressure (mm Hg)	127 ± 15
Diastolic blood pressure (mm Hg)	67 ± 9
Mean cerebral blood flow velocity (cm/second)	45 ± 12
Pulse pressure (mm Hg)	60 ± 13
Pulsatility index	0.97 ± 0.3
LF BP variability (mm Hg)^2	39.5 ± 32.8
LF BFV variability (cm/second)^2	17.9 ± 17
LF coherence	0.51 ± 0.16
LF gain (cm/second per mm Hg)	0.63 ± 0.28
LF phase (rads)	0.99 ± 0.65
HF BP variability (mm Hg)^2	5.4 ± 12.9
HF BFV variability (cm/second)^2	3.6 ± 4.5
HF coherence	0.56 ± 0.14
HF gain (cm/second per mm Hg)	0.93 ± 0.44
HF phase (rads)	0.78 ± 0.8

ACE, angiotensin-converting enzyme; BFV, cerebral blood flow velocity; BP, blood pressure; HF, high frequency (0.16 to 0.5 Hz); ICV, intracranial volume; LF, low frequency (0.03 to 0.15 Hz); NAWM; normal-appearing white matter; WM, cerebral white matter.

Magnetic Resonance Image Acquisition

All participants were imaged using a Siemens Trio 3 Tesla system (Erlangen, Germany) employing a 12-channel phased-array head coil for reception and body coil for transmission. Diffusion-weighted images were obtained using twice-refocused spin echo: 64 slices, TR/TE = 7,920/83 milliseconds, 2-mm isotropic voxels, 60 directions, b = 700 seconds/mm^2, with 10 volumes at *b*-values of zero. A three-dimensional (3D) anatomical scan was acquired using multi-echo MPRAGE with 1 mm isotropic resolution, TR = 2,530 milliseconds, TI = 1000 milliseconds, TE = 1.64, 3.50; 5.36, and 7.22 milliseconds, field of view = 256 × 256 mm (sagittal), matrix size = 256 × 256 × 176, bandwidth = 651 Hz/pixel, and acceleration factor = 2 (GRAPPA). Multispectral white matter lesion segmentation was performed using this T1 image in combination with T2 and proton density weighted images (T2-SPACE; 1 mm isotropic resolution, TR = 3,200 milliseconds, TE = 454 milliseconds, FOV = 256 × 256 mm, matrix size = 256 × 256 × 176 mm, bandwidth = 651 Hz/Px acceleration factor PE = 2 (GRAPPA); MEFLASH: voxel size: 1.5 × 1.5 × 1.5 mm, TR = 70 milliseconds, TEs: 1.6 milliseconds to 67.17 milliseconds (all 24 echo bandwidths = 650 Hz/Px), FOV = 140 × 200 mm (sagittal), matrix size = 140 × 200 × 159 mm, acceleration factor PE = 3 (GRAPPA).

Magnetic Resonance Image Analysis

White matter hyperintensities were measured with FreeSurfer (http://www.surfer.nmr.mgh.harvard.edu) using a multispectral procedure that classifies white matter as normal or abnormal from signal intensities from the T1, PD, and T2 images at each voxel. The FreeSurfer procedure for lesion segmentation is a newly developed procedure that combines the initial standard segmentation with an extension of the subcortical segmentation procedure that incorporates information from a co-registered T2 and PD image for the segmentation of signal abnormalities within the white matter. Although the procedure with T1-weighted images alone tends to underestimate white matter lesion volumes, the incorporation of information from T2/PD provides more robust estimation of the lesion volumes. This WMH segmentation procedure is an extension of a previously described segmentation method.[19] The multiple image modalities were registered to the T1 with boundary-based registration (BBR) and the segmentation of WMH from healthy WM was accomplished with a multispectral Gaussian classifier for each subject based on the atlas values.

Diffusion tensor imaging data were motion and Eddy-current corrected, and subsequently used in computing FA and MD with the FSL Diffusion Toolbox. Maps for FA were entered in voxel-based analyses using the Tract Based Spatial Statistics procedure for inter participant spatial normalization.[20] The Tract Based Spatial Statistics procedure creates a mean FA image by averaging all participants' aligned FA maps and then thresholding this average for voxels with a FA ⩾ 0.2 to generate a mean FA skeleton, which represents the centers of all tracts common to the group. Using this FA skeleton helps exclude regions that are likely composed of multiple tissue types as a result of crossing fibers or fiber orientations that may be susceptible to partial volume contamination. Global FA values using this procedure have demonstrated a range of effects that are minimally confounded.[21]

The region of interest procedure is explained in detail elsewhere.[21] Region of interest was based on the Tract Based Spatial Statistics skeleton and was generated using the John Hopkins University white matter labels available as part of the FSL suite and the T1-based white matter parcellation, which is automatically created during the FreeSurfer processing stream. The region of interest template was co-registered with each subject's diffusion skeleton to obtain white matter parcellation unique to each individual's anatomy. Freesurfer bbregister tool was used to register the T1 image to the lowb volume. Region of interest for the white matter was extracted from native voxels limited to the Tract Based Spatial Statistics FA skeleton to minimize the confounding effect of partial volume contamination on the regional measurements. With this procedure, localized FA measures are based fully on volume of white matter labeled by gyral anatomy and FA values within these localized regions are fairly uniform. The whole brain was then parceled into three

regions based on the vascular territories as follows: (1) regions supplied by the middle cerebral artery (MCA regions), (2) regions not supplied by the MCA (non-MCA regions), and (3) total white matter (global).[22]

Instrumentation

Subjects reported to the Cerebrovascular Laboratory at the Hebrew SeniorLife Institute for Aging Research or General Clinical Research Center at Brigham and Women's Hospital and were instrumented with three lead ECG for continuous heart rate recording. Beat-to-beat arterial blood pressure recordings were obtained using a finger photoplethysmographic cuff (Finometer, Finapres Medical Systems, Amsterdam, The Netherlands). The Finometer transducer was calibrated and the height sensor was zeroed and placed on the finger cuff at heart level with a sling. A 2 MHz transcranial Doppler ultrasonography transducer (MultiDop X4, DWL-Transcranial Doppler Systems, Sterling, VA, USA) was placed on each side of the head and was used to measure the right and left beat-to-beat MCA blood flow velocities. The MCAs were insonated and recorded at a depth of 50 to 60 mm using a Mueller–Moll probe fixation device.[23] All measurements were obtained continuously for 5 minutes while subjects were seated upright in a chair.

Data Analysis

All data were displayed and digitized in real time at 500 Hz with data acquisition software (Windaq, Dataq Instruments, Akron, OH, USA). The blood pressure and cerebral blood flow velocity waveforms were visually inspected for artifacts and ectopy, and only steady-state data were used for analysis. Mean (MAP), systolic, and diastolic (DBP arterial pressures were determined from the mean, maximum, and minimum values of the blood pressure waveforms using a custom software program written in Matlab (Mathworks, Natick, MA, USA). Mean (MFV), systolic and diastolic (DFV) flow velocities were determined from the mean, maximum, and minimum cerebral blood flow velocity within each cycle. Global MFV, systolic flow velocities, and DFV were estimated by averaging the cerebral blood flow velocity variables obtained for the right and the left sides and were used for analysis. Pulse pressure was calculated as the difference between systolic arterial blood pressure and DBP. Pulsatility index was computed as (SFV–DFV)/MFV. Mean hemodynamic variables were obtained by averaging 5-minute steady-state data.

Dynamic Cerebral Autoregulation

Prior studies have established that the frequency-domain transfer function analysis is a valid method for examining dCA.[24,25] This method examines the relationship between the spontaneous beat-to-beat fluctuations in MAP and MFV observed at rest. The arterial blood pressure and right and left cerebral blood flow velocity waveforms obtained at 500 Hz were resampled to 5 Hz and low pass filtered with a cutoff of 0.4 Hz to provide the mean values. The power spectral densities for MAP and MFV were calculated by the Welch average modified periodogram method. The waveforms were linearly detrended, smoothed through a Hanning Window, and transformed through Fast Fourier analysis.[26] The power spectral estimates were averaged across all windows. The cross spectrum between MAP and MFV signals was calculated and used to determine coherence, transfer function phase and gain. Confidence intervals and precisions of estimates for phase and gain were derived based on the level of coherence from standard random theory.[27] The phase and gain values were weighted by their precision to obtain the most accurate means for statistical analysis. By using this method, unreliable estimates with lower coherence received appropriately small weight compared with those with higher coherence accounting for the uncertainty of estimates that may arise from the spontaneous fluctuations.[28] The weighted phase and gain estimates were averaged across each frequency to obtain the group average, which was used for subsequent analyses.

The frequency domain analysis examines the relationship between the spontaneous beat-to-beat fluctuations in MAP and MFV observed at rest. The cross spectrum between MAP and MFV signals are used to determine coherence, phase and gain of the transfer function. The phase shift reflects the temporal difference between transmissions of oscillation from MAP to MFV. If the oscillations of MFV and MAP are almost synchronous, the phase shift approaches zero, which implies impaired dCA and higher phase represents better dCA. Gain, however, is the magnitude of transmission of MAP oscillations to MFV. Effective dCA dampens the transmission of low-frequency MAP oscillations onto MFV. Therefore, lower gain in the low-frequency range can be interpreted as effective dCA. The coherence varies between 0 and 1, and similar to a correlation coefficient, it expresses the fraction of MFV signal that is linearly associated with MAP in the frequency domain. The transfer function phase, gain and coherence were calculated for low (LF, 0.03 to 0.15 Hz) and high (HF, 0.16 to 0.5 Hz) frequency ranges. As dCA can take $\sim$2 to 10 seconds to engage, frequency domain analysis of dCA is typically studied at frequency ranges $\leqslant$0.15 Hz; however, the measures are reported for the entire frequency spectrum.[29] We did not observe a difference between the right and left transfer function parameters; therefore, values from both sides were averaged and the global values were reported.

Statistical Analysis

Subject characteristics were summarized using mean and standard deviation for the continuous variables and frequency distribution for the categorical variables. A weighted multivariable linear regression model was used to analyze the association between dCA and PI as predictors and three different continuous MRI measurement outcomes (WMH with intracranial volume normalization, FA and MD in NAWM). Separate analyses were performed for each MRI outcome with all the predictors adjusted for age, gender, race, diabetes, and hypertension. To account for multiple comparisons, an alpha level of 0.01 was used to determine statistical significance. Subjects were also divided into two groups based on their median score for FA and MD in NAWM. A non-parametric Wilcoxon two-sample test was performed for each FA and MD groups to examine the difference in phase and gain between each group. Spearman rank correlation coefficients were also performed to analyze the association between dCA and FA in the MCA-supplied territory, non-MCA supplied territories, and the whole brain. All statistical analyses were conducted using SAS version 9.2 (SAS Institute, Cary, NC, USA).

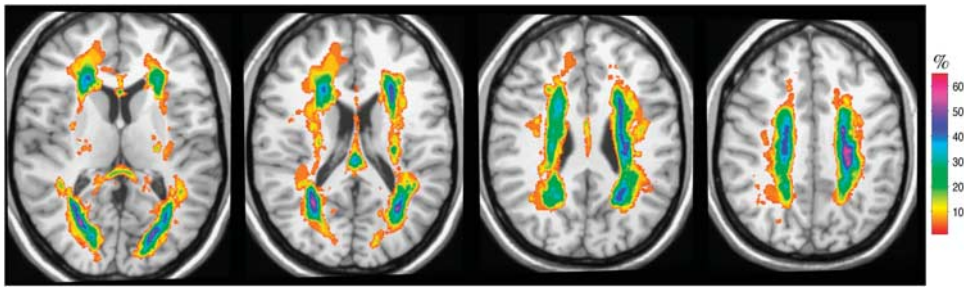

Figure 1. Distribution and frequency of white matter hyperintensities (WMH). The figure visually illustrates the distribution and frequency of WMH obtained from brain images of all subjects. The map was obtained after normalization of all the individual WMH maps to a common space (a reference brain described previously[1]). The WMH frequency map (color) is shown overlaid onto a reference brain (gray scale). The colors represent the percentage (%) of subjects with WMH at a given anatomic location. The color code is illustrated by the color bar on the right. Panels show four different levels (slices), each 10 mm apart in axial view (left to right: more superior parts of the brain). Top and bottom of figure correspond to anterior and posterior of the brain, respectively. The results show a predominantly periventricular distribution of the WMH, especially around the anterior and posterior horns of the ventricles. In some cases, WMH is also present in deep white matter areas.

RESULTS

In this study, 85% of the subjects were white, 42% diabetic, and 70% hypertensive with reasonably well-controlled blood pressures as measured on the study day (Table 1). Cerebrovascular hemodynamic variables were comparable with previously reported values for this age group.[30] In our study, WMH was predominantly observed in the periventricular regions, especially around the anterior and posterior horns of the ventricles (Figure 1). In some individuals, WMH was also evident in the deep white matter regions.

Cerebrovascular Hemodynamics and Global Cerebral White Matter Structural Integrity

Pulsatility index was associated with WMH but not with DTI measures (FA and MD) in NAWM. Individuals with higher PI (lower cerebrovascular compliance) had a larger volume of WMH ($P<0.005$). There was no relationship between MAP or Pulse pressure and WMH volume, FA or MD (Table 2).

Measures of dCA in the LF range were primarily associated with FA and MD (Table 2). Higher phase (better dCA) in the LF range was associated with higher FA ($P<0.001$) and lower MD (greater structural integrity) in NAWM ($P=0.005$). Lower gain in the LF range (better dCA) was also associated with higher FA in NAWM ($P=0.001$). The relationship for phase were also observed in the HF range where higher phase was associated with higher FA ($P<0.001$) and lower MD in NAWM ($P<0.001$). Similar relationship between LF and HF phase and FA were also observed in the regions of WMH (Supplementary Table 3). For the majority of oscillations across the entire frequency range, phase and gain measures indicated better dCA in individuals with higher FA

Table 2. Associations between measures of cerebral white matter structural integrity and physiologic measures

	Estimate (CI_{95})		
	White matter hyperintensity normalized by ICV (%)	*Fractional anisotropy in NAWM*[a]	*Mean diffusivity in NAWM*[a]
Mean arterial pressure (mm Hg)	-7.7×10^{-4} (−0.03, 0.024)	0.2 (−1.2, 1.6)	−0.14 (−0.22, 1.9)
Pulse pressure (mm Hg)	−0.01 (−0.03, 0.01)	−0.13 (−1.2, 0.9)	0.37 (−1.2, 1.9)
Pulsatility index	1.25* (0.41, 2.09)	7.9 (−60.5, 44.8)	16.6 (−58.7, 92.1)
LF gain (cm/second per mm Hg)	−0.21 (−1.11, 0.68)	−84.2* (−130, −39)	58.8 (−14.8, 132)
LF phase (rads)	−0.44 (−0.82, −0.05)	37.8* (18, 56)	−42.6* (−72, −13)
HF gain (cm/second per mm Hg)	0.09 (−0.44, 0.64)	−46.8* (−76, −17)	20 (−28, 67)
HF phase (rads)	−0.41* (−0.72, −0.11)	50.6* (38, 63)	−53* (−77, −29)

CI, confidence interval; HF, high frequency (0.16 to 0.5 Hz); ICV, intracranial volume; NAWM: normal-appearing white matter; LF, low frequency (0.03 to 0.15 Hz). All values represent beta coefficients and 95% confidence interval (CI_{95}) obtained from multi variable linear regression model adjusted for age, gender, race, diabetes, and hypertension. *P value <0.01. [a]Expressed as 10^{-3} for ease of presentation.

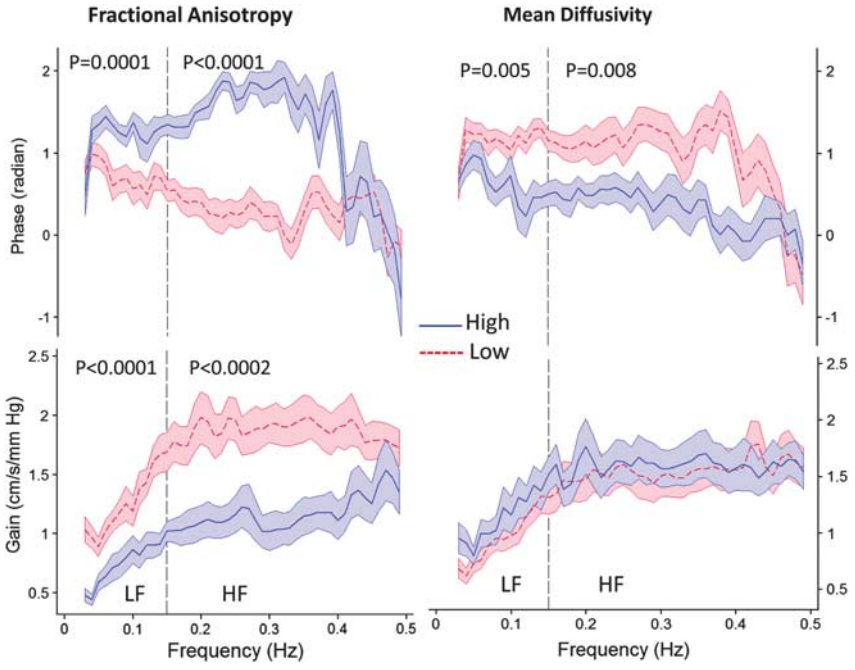

Figure 2. Relationship between dynamic cerebral autoregulation and fractional anisotropy (FA) and mean diffusivity (MD) in normal-appearing white matter. Transfer function phase and gain are plotted across the frequency spectrum of 0 to 0.5 Hz in subjects with low and high (divided at the median) fractional anisotropy (FA, median = 0.395, range = 0.319 to 0.478) and mean diffusivity (MD, median = 0.814, range = 0.716 to 1.061) in regions of normal-appearing white matter. Solid blue and dashed red lines indicate mean phase and gain across the frequency range for high and low FA and MD, respectively, and the shaded regions are standard error of the mean (s.e.m.). Low FA and high MD represent lower white matter structural integrity and lower phase and higher gain values indicate less effective dynamic cerebral autoregulation.

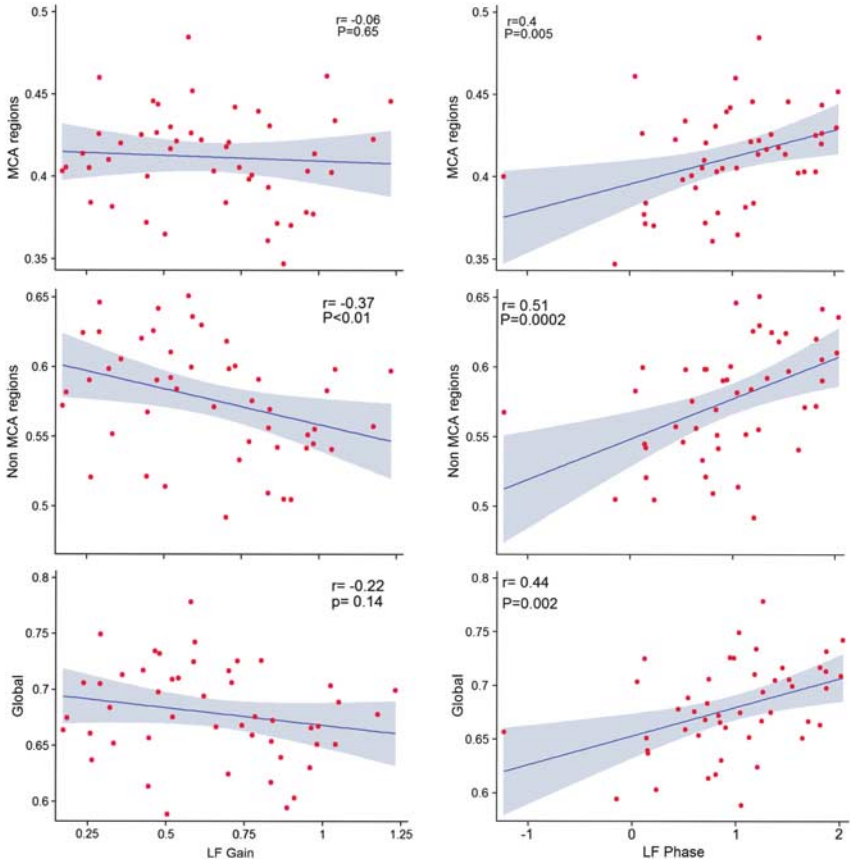

Figure 3. Relationship between dynamic cerebral autoregulation and fractional anisotropy in normal-appearing white matter in the middle cerebral artery territory and whole brain. Scatterplots illustrate the relationship between transfer function phase or gain and fractional anisotropy in normal-appearing white matter supplied by the middle cerebral artery (MCA region), normal-appearing white matter not supplied by the MCA (non-MCA regions) and the whole brain normal-appearing white matter (Global). The shaded region in each graph represents the 95% confidence intervals of the linear prediction line. r = correlation coefficient; P = alpha level of significance.

(Figure 2). Phase, but not gain, was also related to MD for the majority of the frequency range. There was no significant relationship between measures of dCA (phase and gain) and WMH volume.

Cerebrovascular Hemodynamics and Regional Cerebral White Matter Structural Integrity

We also examined the relationship between dCA and white matter structural integrity in the MCA-supplied territory (Figure 3). Similar to our white matter analysis across the entire brain, we found a strong relationship between phase in the LF region and FA in the NAWM in the MCA and non-MCA supplied territories. We did not find any relationship between gain and FA. None of the measures of dCA were associated with MD in the MCA territory (data not shown).

DISCUSSION

Our study shows that impaired cerebrovascular hemodynamics are associated with cerebral white matter injury in elderly individuals with vascular risk factors. Dynamic cerebral autoregulation was less effective in individuals with greater damage in NAWM and cerebrovascular compliance was lower in individuals with greater volume of WMH. Our findings provide additional support linking cerebrovascular impairment to cerebral white matter injury. Understanding the relationship between dCA and white matter structural integrity early in the course of white matter damage, at a time when interventions might be most effective, may lead to new therapeutic targets for the prevention and treatment of white matter disease.

In this study, the most robust relationship was between the phase and FA in NAWM. This relationship persisted across all frequencies and in both the regional (MCA territory only) and global (whole brain) analysis. In fact, previous studies utilizing transfer function analysis for the assessment of dCA have shown that phase may be a much more sensitive measure of dCA than gain.[29] Similarly, because MD measures average diffusion across each voxel, it may not be sensitive to subtle changes in white matter microstructure. In support of this, a recent study demonstrated that unlike the FA metric, MD was not associated with development of WMH as estimated from growing and *de novo* WMH volumes.[15] Therefore, our finding, which shows a strong relationship between dCA and early white matter injury, is also physiologically supported by prior studies, which identify phase of dCA and FA in NAWM as sensitive measures of autoregulation and white matter structural integrity, respectively.

As we were most interested in understanding the relationship between cerebrovascular hemodynamics and early white matter changes, we limited our DTI analysis to the NAWM. The early changes in the NAWM, which constitutes the largest white matter component of the brain in most individuals, including those with severe WMH, may have a greater impact on cerebral function than the WMH volumes.[31] A recent study

showed that structural abnormalities in NAWM increased with WMH severity and DTI metrics were strongly associated with cognitive dysfunction.[32] Non-invasive physiologic measures, such as dCA, which are associated with early white matter injury, will help us identify individuals at a higher risk of white matter injury and its clinical consequences of motor and cognitive decline before the development of WMH. However, non-invasive dCA measures will need to be validated in normal control subjects across all ages before they can be used to detect early white matter injury.

Surprisingly, we did not find a relationship between dCA and the volume of WMH. As reported by others, WMH volume was strongly correlated with PI.[10,33] Those with a lower arterial compliance (higher PI) also had higher volume of WMH. There was no relationship between DTI measures and PI. Given the range of pathologic changes seen in white matter injury, one possible explanation may be that WMH and DTI measures represent different pathologic processes. Alternatively, there may be different stages of the same pathologic process. It may be that white matter shrinkage and formation of WMH follow microstructural deterioration so that early in the course, autoregulation may be impaired, but with progressive vascular and white matter damage autoregulation becomes completely disabled and the cerebrovascular tree loses all its compliance.

Finally, it is also important to note that we did not observe a relationship between MAP or PP and WMH. The most likely explanation is that the majority of participants in this study were well-controlled hypertensive within a very narrow age and blood pressure range. It has also been shown that progression of WMH is slowed in well-controlled hypertensive participants suggesting a potential benefit of treatment.[34] Prior studies that have shown a link between blood pressure and white matter injury have included a diverse age group of hypertensive participants with various levels of blood pressure control.[35–37]

Our study is limited by its cross-sectional design, which prevents us from assuming any causal relationship between impairment in cerebral hemodynamics and cerebral white matter injury. Future longitudinal studies are needed to better understand the relationships reported in our study. Second, dCA was only measured in the MCA territory, and we do not have measures of autoregulation in other vascular territories. However, we found that dCA in the MCA territory was not only related to global DTI measures, but also to the MCA and non-MCA territory DTI measures as well. Our findings suggest that dCA in the MCA territory, which is the largest vascular territory in the brain, may be a reasonable measure of global dCA. However, this hypothesis will need to be confirmed by future studies with simultaneous dCA measures in the anterior, middle, and posterior cerebral arteries.

In summary, we show that in elderly individuals with vascular risk factors, impaired cerebrovascular hemodynamics are associated with cerebral white matter injury. Dynamic cerebral autoregulation is strongly correlated with loss of structural integrity in NAWM and reduced cerebrovascular compliance is associated with WMH. The different patterns of cerebrovascular hemodynamics in NAWM and WMH may represent different pathologic process or could represent different stages of the same pathology.

DISCLOSURE/CONFLICT OF INTEREST

The authors declare no conflict of interest.

REFERENCES

1 Moscufo N, Guttmann CR, Meier D, Csapo I, Hildenbrand PG, Healy BC *et al.* Brain regional lesion burden and impaired mobility in the elderly. *Neurobiol Aging* 2011; **32**: 646–654.
2 de Laat KF, van Norden AG, Gons RA, van Oudheusden LJ, van Uden IW, Norris DG *et al.* Diffusion tensor imaging and gait in elderly persons with cerebral small vessel disease. *Stroke* 2011; **42**: 373–379.
3 de Laat KF, Tuladhar AM, van Norden AG, Norris DG, Zwiers MP, de Leeuw FE. Loss of white matter integrity is associated with gait disorders in cerebral small vessel disease. *Brain* 2011; **134**: 73–83.
4 Kalaria RN. Cerebrovascular disease and mechanisms of cognitive impairment: evidence from clinicopathological studies in humans. *Stroke* 2012; **43**: 2526–2534.
5 Farkas E, de Vos RA, Donka G, Jansen Steur EN, Mihaly A, Luiten PG. Age-related microvascular degeneration in the human cerebral periventricular white matter. *Acta Neuropathol* 2006; **111**: 150–157.
6 Fernando MS, Simpson JE, Matthews F, Brayne C, Lewis CE, Barber R *et al.* White matter lesions in an unselected cohort of the elderly: molecular pathology suggests origin from chronic hypoperfusion injury. *Stroke* 2006; **37**: 1391–1398.
7 Gouw AA, Seewann A, van der Flier WM, Barkhof F, Rozemuller AM, Scheltens P *et al.* Heterogeneity of small vessel disease: a systematic review of MRI and histopathology correlations. *J Neurol Neurosurg Psychiatry* 2011; **82**: 126–135.
8 Gunning-Dixon FM, Brickman AM, Cheng JC, Alexopoulos GS. Aging of cerebral white matter: a review of MRI findings. *Int J Geriatr Psychiatry* 2009; **24**: 109–117.
9 Birns J, Jarosz J, Markus HS, Kalra L. Cerebrovascular reactivity and dynamic autoregulation in ischaemic subcortical white matter disease. *J Neurol Neurosurg Psychiatry* 2009; **80**: 1093–1098.
10 Mok V, Ding D, Fu J, Xiong Y, Chu WW, Wang D *et al.* Transcranial Doppler ultrasound for screening cerebral small vessel disease: a community study. *Stroke* 2012; **43**: 2791–2793.
11 Poels MM, Zaccai K, Verwoert GC, Vernooij MW, Hofman A, van der Lugt A *et al.* Arterial stiffness and cerebral small vessel disease: the rotterdam scan study. *Stroke* 2012; **43**: 2637–2642.
12 Moody DM, Brown WR, Challa VR, Ghazi-Birry HS, Reboussin DM. Cerebral microvascular alterations in aging, leukoaraiosis, and Alzheimer's disease. *Ann N Y Acad Sci* 1997; **826**: 103–116.
13 Brown WR, Moody DM, Challa VR, Thore CR, Anstrom JA. Venous collagenosis and arteriolar tortuosity in leukoaraiosis. *J Neurol Sci* 2002; **203-204**: 159–163.
14 Maillard P, Carmichael O, Harvey D, Fletcher E, Reed B, Mungas D *et al.* FLAIR and diffusion MRI signals are independent predictors of white matter hyperintensities. *AJNR Am J Neuroradiol* 2013; **34**: 54–61.
15 de Groot M, Verhaaren BF, de Boer R, Klein S, Hofman A, van der Lugt A *et al.* Changes in normal-appearing white matter precede development of white matter lesions. *Stroke* 2013; **44**: 1037–1042.
16 Salat DH, Tuch DS, Greve DN, van der Kouwe AJ, Hevelone ND, Zaleta AK *et al.* Age-related alterations in white matter microstructure measured by diffusion tensor imaging. *Neurobiol Aging* 2005; **26**: 1215–1227.
17 Joutel A, Monet-Lepretre M, Gosele C, Baron-Menguy C, Hammes A, Schmidt S *et al.* Cerebrovascular dysfunction and microcirculation rarefaction precede white matter lesions in a mouse genetic model of cerebral ischemic small vessel disease. *J Clin Invest* 2010; **120**: 433–445.
18 Budde MD, Kim JH, Liang HF, Schmidt RE, Russell JH, Cross AH *et al.* Toward accurate diagnosis of white matter pathology using diffusion tensor imaging. *Magn Reson Med* 2007; **57**: 688–695.
19 Fischl B, Salat DH, Busa E, Albert M, Dieterich M, Haselgrove C *et al.* Whole brain segmentation: automated labeling of neuroanatomical structures in the human brain. *Neuron* 2002; **33**: 341–355.
20 Smith SM, Jenkinson M, Johansen-Berg H, Rueckert D, Nichols TE, Mackay CE *et al.* Tract-based spatial statistics: voxelwise analysis of multi-subject diffusion data. *Neuroimage* 2006; **31**: 1487–1505.
21 Salat DH, Williams VJ, Leritz EC, Schnyer DM, Rudolph JL, Lipsitz LA *et al.* Inter-individual variation in blood pressure is associated with regional white matter integrity in generally healthy older adults. *Neuroimage* 2012; **59**: 181–192.
22 Haines DE. *Neuroanatomy an Atlas of Structures, Sections, and Systems*. 8 edn. Lippincott Williams & Wilkins: Philadelphia, 2011.
23 Aaslid R, Markwalder TM, Nornes H. Noninvasive transcranial Doppler ultrasound recording of flow velocity in basal cerebral arteries. *J Neurosurg* 1982; **57**: 769–774.
24 Panerai RB, Rennie JM, Kelsall AW, Evans DH. Frequency-domain analysis of cerebral autoregulation from spontaneous fluctuations in arterial blood pressure. *Med Biol Eng Comput* 1998; **36**: 315–322.
25 Zhang R, Zuckerman JH, Levine BD. Spontaneous fluctuations in cerebral blood flow: insights from extended-duration recordings in humans. *Am J Physiol Heart Circ Physiol* 2000; **278**: H1848–H1855.
26 Hamner JW, Tan CO, Lee K, Cohen MA, Taylor JA. Sympathetic control of the cerebral vasculature in humans. *Stroke* 2010; **41**: 102–109.
27 Koopmans LH. *The Spectral Analysis of Time Series*. 2nd edn (Academic Press: New York, 1995.
28 Searle SR. *Linear Models for Unbalanced Data*. Wiley: New York, 1987.

29 Panerai RB. Cerebral autoregulation: from models to clinical applications. *Cardiovasc Eng* 2008; **8**: 42–59.
30 Sorond FA, Galica A, Serrador JM, Kiely DK, Iloputaife I, Cupples LA *et al.* Cerebrovascular hemodynamics, gait, and falls in an elderly population: MOBILIZE Boston Study. *Neurology* 2010; **74**: 1627–1633.
31 Fazekas F, Wardlaw JM. The origin of white matter lesions: a further piece to the puzzle. *Stroke* 2013; **44**: 951–952.
32 Schmidt R, Ropele S, Ferro J, Madureira S, Verdelho A, Petrovic K *et al.* Diffusion-weighted imaging and cognition in the leukoariosis and disability in the elderly study. *Stroke* 2010; **41**: e402–e408.
33 Webb AJ, Simoni M, Mazzucco S, Kuker W, Schulz U, Rothwell PM. Increased cerebral arterial pulsatility in patients with leukoaraiosis: arterial stiffness enhances transmission of aortic pulsatility. *Stroke* 2012; **43**: 2631–2636.
34 Godin O, Tzourio C, Maillard P, Mazoyer B, Dufouil C. Antihypertensive treatment and change in blood pressure are associated with the progression of white matter lesion volumes: the Three-City (3C)-Dijon Magnetic Resonance Imaging Study. *Circulation* 2011; **123**: 266–273.
35 de Leeuw FE, Richard F, de Groot JC, van Duijn CM, Hofman A, Van Gijn J *et al.* Interaction between hypertension, apoE, and cerebral white matter lesions. *Stroke* 2004; **35**: 1057–1060.
36 Sierra C, de la Sierra A, Chamorro A, Larrousse M, Domenech M, Coca A. Cerebral hemodynamics and silent cerebral white matter lesions in middle-aged essential hypertensive patients. *Blood Press* 2004; **13**: 304–309.
37 van Dijk EJ, Breteler MM, Schmidt R, Berger K, Nilsson LG, Oudkerk M *et al.* The association between blood pressure, hypertension, and cerebral white matter lesions: cardiovascular determinants of dementia study. *Hypertension* 2004; **44**: 625–630.

Supplementary Information accompanies the paper on the Journal of Cerebral Blood Flow & Metabolism website (http://www.nature.com/jcbfm)